FAST NEUTRON THERMALIZATION AND CAPTURE GAMMA-RAY GENERATION IN SOILS

S.L. Shue, R.E. Faw, and J.K. Shultis, Department of Nuclear Engineering, Kansas State University, Manhattan, KS, 66506

ABSTRACT The penetration of 14-MeV neutrons into five representative soils is investigated with two independent neutron transport calculational procedures. From Monte Carlo and discrete-ordinates codes, the spatial distribution of the thermal fluence and the capture of neutrons in the soils is determined for two neutron source geometries. Finally, empirical approximations of the thermal neutron fluence in the soil are presented for use in PGNAA of contaminants in the soil.

KEYWORDS: PGNAA, soil, neutron fluence, capture gamma-rays, activation

INTRODUCTION

The method of prompt gamma-ray neutron activation analysis (PGNAA) is potentially a powerful method for non-invasive and rapid determination of vertical contaminant profiles in soil. In this method, fast neutrons are directed into the soil from a plane-parallel beam or from an isotropic point source on the surface. A collimated radiation detector above the soil then measures the intensities of the characteristic gamma rays released by elements in the soil that capture the neutrons. Analytical procedures for "de-convoluting" or inverting the measured gamma-ray spectra are then applied to estimate contaminant concentration profiles.

Crucial to estimating a contaminant profile from the measured intensities of the capture gamma-photons is an accurate knowledge of the neutron field in the soil and the spatial distribution of neutron absorptions by the contaminant. This paper calculates the energy dependent neutron fluence distribution in five representative soils for two neutron source geometries. From these calculated fluence distributions, we show how the capture gamma-ray source strength in the soils can be calculated accurately using only the thermal-neutron fluence profiles. This capture gamma-ray source strength is critical *a priori* information needed for estimating the contaminant profile from the measured data.

The first neutron source geometry considered is very simple and one-dimensional. A plane parallel beam of 14-MeV neutrons is normally incident on the soil surface with intensity J_o per cm^2. The neutron source energy of 14 MeV is based on the fusion reaction induced by accelerated deuterons striking a tritiated target. This is a standard source of fast neutrons, employing a Cockroft-Walton accelerator with an accelerating potential of about 150 keV. The energy spectrum of the neutron fluence $\Phi(z,E)$ is computed as a function of depth z in the soil and the fluence is normalized as $\ddot{\Phi} = \Phi / J_o$. Also computed is the capture of neutrons in soil contaminants such as heavy-metal elements. For unit atomic concentration of element j in the soil, the capture may be expressed as

$$A_j(z) = \int dE \Phi(z,E) \sigma_c^j(E), \qquad (1)$$

in which $\sigma_c^j(E)$ is the cross section for radiative capture of a neutron of energy E by an atom of element j. This quantity may also be normalized as $A_j = A_j / J_o$. This one-dimensional geometry, while not physically realistic, establishes the framework for a very straightforward, easily explained, and easily modeled set of reference calculations [1].

The second source geometry considered models a commercial unit [2-5] developed for field application of the PGNAA technique of soil assay. This geometry involves a point isotropic source emitting S_o neutrons placed 15 cm above the surface of the soil. The neutron transport calculations are thus two-dimensional if axisymmetric cylindrical coordinates are used. The energy spectrum of the neutron fluence $\Phi(r, z, E)$ is computed as a function of two coordinates, namely the depth z in the soil and the radial distance r from a line from the source normal to the soil surface. The fluence is normalized as $\dot{\Phi} = \Phi / S_o$. Also computed is the capture of neutrons in soil contaminants as in the case of the beam source.

Two methods of performing neutron transport calculations are used in this study. One is the MCNP code [6] based on the Monte Carlo method. This is an industry standard widely used to perform benchmark calculations to gauge the performance of other codes. Monte Carlo calculations closely model physical reality. However, they are not suited for deep-penetration transport problems of the type needed in this study. More suited to deep-penetration problems are codes based on the discrete ordinates method. One such code, the TORT code [7] developed at Oak Ridge National Laboratory, was the initial choice for use in this investigation and was used for three-dimensional calculations. A newly-released code, DANTSYS [8-11], developed at Los Alamos National Laboratory, was found to be more suitable for the two-dimensional calculations and was also used to verify the one-dimensional calculations. As is discussed in subsequent sections, some of the computational methods are based not on continuous distributions in energy, but on a multigroup distribution, such that Φ_g is the neutron fluence in energy group g, which has upper and lower limits respectively given by E_g and E_{g+1}.

ELEMENTAL SOIL COMPOSITIONS

The earth's crust is composed of both rock and weathered rock (soil). Weathering can be broken into two broad categories: mechanical and chemical. Seasonal weather changes can mechanically break down rocks into increasingly smaller pieces and eventually into the individual minerals. Chemical weathering can cause changes in mineral composition by hydrolysis, hydration, oxidation, and carbonation. The principal minerals exposed to weathering to produce soil are silicates, oxides, and hydroxides of sodium, potassium, iron, calcium, and magnesium.

Soil water content varies greatly. The water in soil can be separated into four categories: chemically-bound, hygroscopic, capillary, and gravitational water. Both chemically-bound and hygroscopic water are closely associated with the soil particles. However, bound water is chemically bound to the mineral while hygroscopic water adheres to the surface. To release the bound water, the soil has to be heated to temperatures in

excess of 600ºC. Hygroscopic water is released at temperatures higher than 110ºC. Capillary water is the water trapped in the pores of the soil, which evaporates when exposed to air. This includes most of the water taken up by growing plants. Capillary water is held in the pores by surface tension. Excess capillary water becomes gravitational water which moves with the force of gravity. It occupies larger pores and can harm growing plants by reducing soil aeration. This water moves downward through the soil, rising again when capillary water is decreased.

For the purpose of this study, water content is divided into bound and free water. Water content is the ratio of the mass of the water to the mass of the dry solids. Bound water includes both chemically-bound and hygroscopic water. Values for the fraction of bound water vary greatly with soil type. Soils high in colloidal materials hold more bound water than do sandy soils and those low in clay and humus. For the present work, a bound water content of 0.05 was chosen. This value is typical of a well-granulated silt loam.

Since free water and air are located in the soil pores, pore size influences soil moisture content and aeration. Pores are divided into micropores and macropores. The micropores in clay allow poor water and air transport, resulting in high water-holding capacity and slow drainage. In sand, the macropores allow rapid water drainage and high aeration. Porosity is defined as the ratio of the volume of air and water to the volume of solids. Optimum soil conditions require a porosity of approximately 0.5. Soil porosity usually varies within the range 0.4 to 0.6. For this study, a normal soil porosity of 0.5 was chosen. Also defined (as extremes) are a porous soil with porosity of 0.4 and a dense soil with porosity of 0.6. In a well-granulated silt loam surface soil at optimum moisture for plant growth, the total pore space is likely to be shared equally by air and free water. Numerous studies led to a decision to use a free water content of 0.2 for normal soil. To account for extremes, values of 0.1 for dry soil and 0.3 for wet soil were chosen.

Soil organic matter represents an accumulation of partially-decayed and synthesized plant and animal residues or humus. The organic component of soil helps to keep the soil well-granulated. Most authorities state that soil contains approximately 5 to 7 percent organic material by volume. Since the organic component of soil is so small and its composition is so varied, its effects are neglected in this study.

It is thus seen that the main factors affecting chemical composition and density are mineral content, water content (both bound and free) and porosity. However, elemental content of the mineral component of dry soil can be assumed to be fairly constant. For this study, the chemical composition of dry soil is taken to be the chemical composition of the earth's crust. Table 1 lists the chemical compositions and densities of the five reference types of soil whose neutron transmission properties are studied in this paper. Additional information about these representative soils is provided by Faw, *et al.* [12].

NEUTRON TRANSPORT METHODOLOGY

In this study two quite different approaches are used to estimate the neutron field in the soil. By using state-of-the-art codes based on the Monte Carlo and the discrete-ordinates methods, results for the same problem calculated with different codes and based on different nuclear data libraries serve as checks on the accuracy of the calculated neutron fields. In the sections following we summarize the methods and data used by these various neutron transport codes.

The Monte Carlo method

The Monte Carlo method of performing radiation transport calculations is very different from analytical or deterministic numerical methods, which require solution of a set of coupled integro-differential equations that are exceedingly difficult to solve. In Monte Carlo calculations, simulated particle tracks are generated by mimicking the random nature of individual particle interactions within the transport medium. It is not even necessary to invoke the transport equation for the more elementary operations. All one needs are complete mathematical expressions of the probability relationships that govern (1) the track length of an individual particle between interaction points, (2) the choice of an interaction type at each such point, (3) the choice of a new energy and a new direction if the interaction is of a scattering type, and (4) the possible production of additional particles. These are all stochastic variables, and in order to make selections of specific values for these variables, one needs a complete understanding of the various processes a particle undergoes in its lifetime

TABLE 1. CHEMICAL COMPOSITIONS AND DENSITIES OF FIVE REPRESENTATIVE SOILS.

	Soil type				
	Nominal	Dry porous	Dry dense	Wet porous	Wet dense
Porosity[a]	0.5	0.6	0.4	0.6	0.4
Free water content[b]	0.2	0.1	0.1	0.3	0.3
Bound water content[c]	0.05	0.05	0.05	0.05	0.05
Mineral density (g/cm^3)[d]	2.684	2.684	2.684	2.684	2.684
In situ density (g/cm^3)	1.6104	1.1810	1.7714	1.3957	2.0935
Element	Weight fraction				
Hydrogen	0.02331	0.01526	0.01526	0.03013	0.03013
Oxygen	0.55921	0.52931	0.52931	0.58451	0.58451
Silicon	0.22259	0.24282	0.24282	0.20547	0.20547
Aluminum	0.06528	0.07122	0.07122	0.06026	0.06026
Iron	0.04015	0.04380	0.04380	0.03706	0.03706
Calcium	0.02915	0.03180	0.03180	0.02691	0.02691
Potassium	0.02080	0.02269	0.02269	0.01920	0.01920
Sodium	0.02272	0.02479	0.02479	0.02098	0.02098
Magnesium	0.01678	0.01831	0.01831	0.01549	0.01549

[a]Fraction of total volume occupied by water and air.
[b]Ratio of free water mass to mineral mass.
[c]Ratio of bound water mass to mineral mass.
[d]Mineral density includes bound water.

from the time it is given birth by the source until it is either absorbed or leaves the system under consideration. The average behavior of particles in the physical is then inferred from the average behavior of the simulated particles.

The process of deciding on a specific value of some stochastic variable is generally based on the selection of a number at random from a uniformly distributed set of integers, say, from 1 to some large maximum number *N*. A simple way to do this might be to use a nonbiased roulette wheel which can be used to pick at random any number from 1 to *N*. This invokes images of gambling at Monte Carlo, hence the name of this method. For our purposes the process is more elaborate and more suited to computing machinery, but the principle is similar.

The experience a particle undergoes from the time it leaves its source until it is absorbed or passes out of the system is called its *history*. The process of using a computer to follow a given number of particle histories can be accomplished in a way completely analogous to the actual physical process of particle transport through a medium. The absorption, escape, or other event associated with each particle may be *scored* or *tallied* in various ways to yield, after all histories are completed, quantities such as angular or energy distributions as well as fluences, flows, or absorbed doses. For example, when a particle passes through a surface, tallies may be incremented in groups or bins associated with the particle's energy and direction cosines, thus permitting calculation of energy and angular distributions of the particle fluence or flow. This direct simulation of the physical situation is called an *analog* Monte Carlo procedure. On the other hand, it is possible to use a Monte Carlo process to solve a problem that is physically much different from the one of basic interest. This is possible under circumstances for which it can be proved that the resulting answer (say, a detector response) to the altered procedure is the same as that for the basic problem, or else has some known relationship to it so that the solution of the basic problem can be obtained indirectly. This use of an associated but altered procedure is called a *nonanalog* Monte Carlo procedure.

In this study, the MCNP general Monte Carlo code [6] is used as the standard against which results of discrete ordinates calculations are compared. The MCNP code may be used for neutron, photon, or electron transport calculations or for coupled calculations involving, for example, creation of gamma rays in neutron interactions, and creation of electrons in gamma-ray interactions. The code may be used in steady or time-dependent problems and in very general three-dimensional geometry. Particle energy is treated on a continuous basis. Neutron energies may vary from 10^{-11} to 20 MeV while photon and electron energies may vary from 1 keV to 1,000 MeV. The primary sources of nuclear data are the Evaluated Nuclear Data File (ENDF), the Evaluated Nuclear Data Library (ENDL), and Activation Library (ACTL) compilations. The MCNP code is distributed and maintained by Los Alamos National Laboratory. It was obtained for use in this research through the auspices of the Radiation Shielding Information Center at Oak Ridge National Laboratory.

The discrete ordinates method

Unlike the Monte Carlo method discussed in the previous section, the discrete ordinates method is based upon an approximation of the neutron transport equation. This approximation is obtained by discretizing the independent variables in the transport equation: direction (**Ω**), energy (E), and space (**r**). The discretization converts the transport equation into a form suitable for further approximation by replacing the derivatives and integrals in the transport equation with their corresponding discrete representations. This results in a set of highly-coupled algebraic equations.

The term *discrete ordinates* specifically refers to the partitioning of all possible directions **Ω**, into a finite or discrete number of directions $\mathbf{\Omega}_m$ [13, 14]. To further simplify the transport equation, both the energy and spatial variables are also discretized. For the energy variable, this involves the so-called multigroup approximation in which the energy range of the neutrons is partitioned into G contiguous subintervals. By convention, the energy groups progress from highest energy (group $g = 1$) to the lowest energy (group $g = G$). The spatial discretization depends upon the choice of coordinate system and the number of dimensions needed to describe the problem. Generally, the spatial partitioning can be thought of as dividing the problem space into intervals, grids, and then cells depending upon the required dimensions. The actual discretization is algebraically intensive and is described fully in the DANTSYS manual [11], the TORT manual [7], and in technical report HSRC-94-02-07 [15].

The discrete ordinates method is a very powerful tool, but extremely intensive in computer memory use. For example, consider a problem containing 10 energy groups, 10 directions, and 10 divisions in x, y, and z. The discrete ordinates method would require the solution of 10^5 simultaneous algebraic equations—a difficult computational task. But, if the necessary computer resources are available, the results are obtained rapidly when compared to other methods such as Monte Carlo.

The discrete ordinates code used in this project is the Diffusion Accelerated Neutral Particle Transport System or DANTSYS. The DANTSYS code is maintained at the Los Alamos National Laboratory in Los Alamos, New Mexico. The code was released in 1995 by R.E. Alcouffe, R.S. Baker, F.W. Brinkley, D.R. Marr, R.D. O'Dell, and W.F. Waters [11].

Neutron transport cross sections

The most general form of the neutron cross section used in the neutron transport calculations is the doubly differential scattering cross section $\sigma(E, E', \omega_s)$, in which E and E' are the neutron energies before and after scattering and ω_s is the cosine of the angle of scattering θ_s. The cross section is defined in such a way that $\sigma(E,E',\omega_s)dE'd\Omega$ is the cross section for an interaction with scattering angle θ_s in $d\Omega$ leaving the scattered neutron with energy E' in dE'. For elastic scattering and most inelastic scattering interactions, conservation of energy and momentum require that the angle of scattering uniquely determines the energy loss. Cross sections are measured in units of cm^2 (per atom), with 1 barn (b) equal to 10^{-24} cm^2. The product of the cross section, the atomic concentration, and the

fluence is the number of interactions of a given type per unit volume.

In Monte Carlo calculations, data are provided for the angular distribution of scattered neutrons as a function of the incident neutron energy. These data are in the form of the singly differential cross section $\sigma(E, \omega_s)$. Random sampling is used to determine the scattering angle, and conservation equations yield the energy after scatter.

In the discrete-ordinates calculations, cross sections are cast into an energy multigroup structure such that the group-to-group transfer cross section is

$$\sigma_{g\to g'}(\omega_s) = \frac{\int_{E_{g+1}}^{E_g} dE W(E) \int_{E_{g'+1}}^{E_{g'}} dE' \sigma(E, E', \omega_s)}{\int_{E_{g+1}}^{E_g} dE W(E).} \qquad (2)$$

in which $W(E)$ is a weight function which approximates the energy spectrum of the neutron fluence. This group-to-group cross section is then approximated by a low-order N-term Legendre polynomial expansion of the form

$$\sigma_{g\to g'}(\omega_s) = \sigma_{g\to g'} \sum_{n=0}^{N} \frac{2n+1}{4\pi} a^n_{g\to g'} P_n(\omega_s), \qquad (3)$$

in which P_n is the nth order Legendre polynomial. The coefficient $a^n_{g\to g'}$ for $n = 0$ is unity and for $n > 0$ is

$$a^n_{g\to g'} = 2\pi \int_{-1}^{1} d\omega_s P_n(\omega_s) \sigma_{g\to g'}(\omega_s). \qquad (4)$$

It is the Legendre expansion coefficient a_n (along with other needed multigroup cross sections) that are provided by the cross section library used by the discrete-ordinates codes. The multigroup cross section data used is this study are from the BUGLE-93 47-group library used by TORT and DANTSYS. They are based on a weight function typical of neutron transport in a concrete medium. The energy group structure for the 47-group BUGLE library is given in Table 2.

Cross sections for neutron attenuation in soil

Fast neutrons interact with elements in the soil by scattering, and by capture or other nuclear reactions. The scattering may be elastic, which releases no secondary photons, or inelastic, which leaves the scattering nucleus in an excited state that is promptly relaxed by emission of a gamma ray. In the radiative capture (n, γ) reaction, primarily a phenomenon experienced by slow neutrons, excess energy of the nucleus is also relaxed by emission of one or more gamma rays. It is radiative capture that permits determination of elemental compositions by analysis of energies of capture gamma rays. Other nuclear reactions include fission and charged particle reactions. A proton reaction, for example, is the ^{28}Si(n, p)^{28}Al reaction. An alpha particle reaction, for example, is the ^{16}O(n, α)^{13}C reaction. Various other reactions such as (n, 2n) and (n, 3n) are possible.

Figures 1 through 3 illustrate cross sections for reactions of key elements in soil. Figure 1 shows the radiative capture cross section and the total cross section, which is the sum of the capture and scattering cross sections. The capture reaction is very important in that with every capture a highly penetrating 2.2-MeV gamma ray is released. The scattering reaction is also very important. For two reasons, hydrogen is the key element in soil most responsible for slowing neutrons. First, the cross section is very high

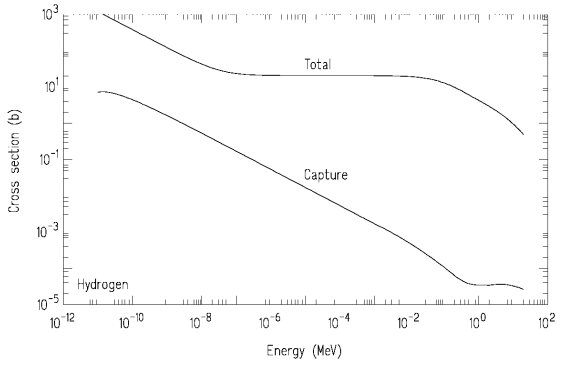

FIGURE 1. THE TOTAL AND $\sigma(n, \gamma)$ CROSS SECTIONS FOR HYDROGEN, DERIVED FROM THE ENDF/B-V DATA SET USED BY THE MCNP CODE. UNITS ARE BARNS = 10^{-24} cm^2.

for scattering, meaning that scattering from hydrogen is highly probable. Second, since the neutron and the hydrogen nucleus have about the same mass, the neutron can lose as much as 100% of its kinetic energy in one scatter; indeed, on average, half the neutron energy is lost in each scatter.

Figures 2 and 3 illustrate total and capture cross sections for oxygen and silicon. The total cross section, primarily for scattering except at very high energies, is nearly constant over a wide range of energies. The capture cross section for oxygen at all energies and the capture cross section for silicon except very high energies show one characteristic nature of capture cross sections that σ_c varies inversely with neutron velocity, i.e., as $E^{-1/2}$. Resonances at high energies account for the structure in the total cross sections for both oxygen and silicon. Resonances may play a role in capture, as is the case for silicon but not for oxygen, in scattering and in charged-particle reactions.

TABLE 2. NEUTRON ENERGY GROUP STRUCTURE FOR THE BUGLE-93 CROSS-SECTION DATA SET USED BY THE TORT AND DANTSYS DISCRETE-ORDINATES RADIATION TRANSPORT CODES. ENERGY UNITS ARE MeV. IN THIS STUDY, 14-MeV (SOURCE) NEUTRONS ARE IN GROUP 2, THERMAL NEUTRONS ARE IN GROUP 47.

g	E_g (MeV)	g	E_g (MeV)	g	E_g (MeV)
1	$1.7332 \times 10^{+01}$	17	1.6530×10^{-00}	33	2.1875×10^{-02}
2	$1.4191 \times 10^{+01}$	18	1.3534×10^{-00}	34	1.5034×10^{-02}
3	$1.2214 \times 10^{+01}$	19	1.0026×10^{-00}	35	7.1017×10^{-03}
4	$1.0000 \times 10^{+01}$	20	8.2085×10^{-01}	36	3.3546×10^{-03}
5	8.6071×10^{-00}	21	7.4274×10^{-01}	37	1.5846×10^{-03}
6	7.4082×10^{-00}	22	6.0810×10^{-01}	38	4.5400×10^{-04}
7	6.0653×10^{-00}	23	4.9787×10^{-01}	39	2.1445×10^{-04}
8	4.9659×10^{-00}	24	3.6883×10^{-01}	40	1.0130×10^{-04}
9	3.6788×10^{-00}	25	2.9721×10^{-01}	41	3.7266×10^{-05}
10	3.0199×10^{-00}	26	1.8316×10^{-01}	42	1.0677×10^{-05}
11	2.7253×10^{-00}	27	1.1109×10^{-01}	43	5.0435×10^{-06}
12	2.4660×10^{-00}	28	6.7379×10^{-02}	44	1.8554×10^{-06}
13	2.3653×10^{-00}	29	4.0868×10^{-02}	45	8.7643×10^{-07}
14	2.3457×10^{-00}	30	3.1828×10^{-02}	46	4.1399×10^{-07}
15	2.2313×10^{-00}	31	2.6058×10^{-02}	47	1.0000×10^{-07}
16	1.9205×10^{-00}	32	2.4176×10^{-02}		1.0000×10^{-12}

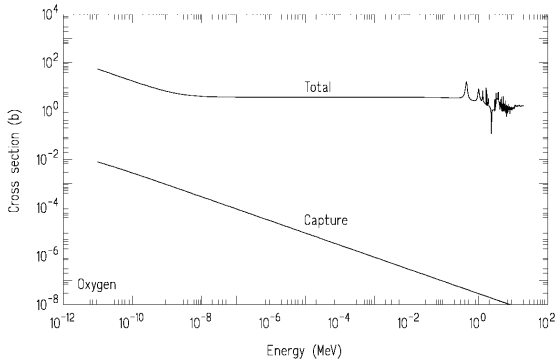

FIGURE 2. THE TOTAL AND $\sigma(n, \gamma)$ CROSS SECTIONS FOR ^{16}O, DERIVED FROM THE ENDF/B-V DATA SET USED BY THE MCNP CODE. UNITS ARE BARNS = 10^{-24} cm^2.

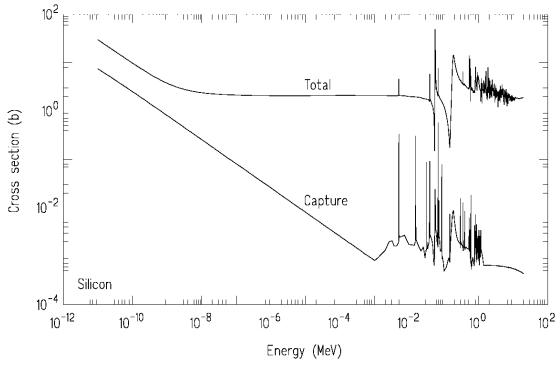

FIGURE 3. THE TOTAL AND $\sigma(n, \gamma)$ CROSS SECTIONS FOR ELEMENTAL SILICON, DERIVED FROM THE ENDF/B-V DATA SET USED BY THE MCNP CODE. UNITS ARE BARNS = 10^{-24} cm^2.

Cross sections for neutron capture reactions

Figures 4 and 5 illustrate neutron capture cross sections as a function of neutron energy for all radiative capture reactions with ^{238}U and with elemental copper. Data in the continuous curves are from the definitive ENDF/B-V compilation. Quite apparent are the many resonances in the cross sections at intermediate energies on the order of 1 keV. A distinctive feature of the MCNP Monte Carlo code is that it makes use of the continuous cross section function in its calculations. Multi-group neutron transport

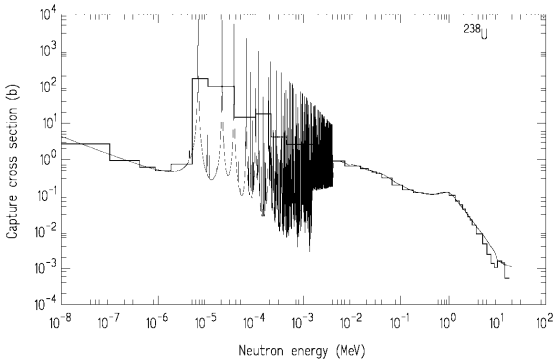

FIGURE 4. THE $\sigma(n, \gamma)$ CROSS SECTIONS FOR ^{238}U FROM THE UNWEIGHTED BUGLE-93 DATA SET USED BY THE TORT AND DANTSYS CODES (HISTOGRAM) AND FROM THE ENDF/B-V DATA SET USED BY THE MCNP CODE (CONTINUOUS LINE). UNITS ARE BARNS = 10^{-24} cm^2.

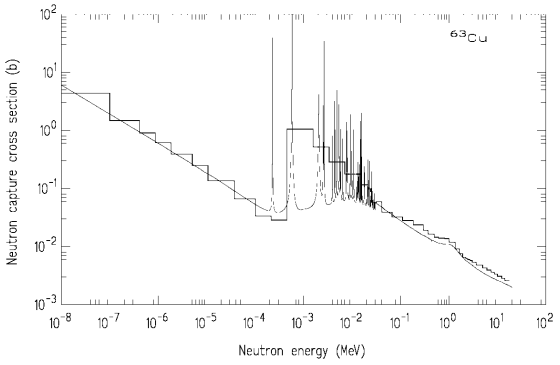

FIGURE 5. THE $\sigma(n, \gamma)$ CROSS SECTIONS FOR ^{63}Cu FROM THE UNWEIGHTED BUGLE-93 DATA SET USED BY THE TORT AND DANTSYS CODES (HISTOGRAM) AND FROM THE ENDF/B-V DATA SET USED BY THE MCNP CODE (CONTINUOUS LINE). UNITS ARE BARNS = 10^{-24} cm^2.

codes, by their nature, require treating neutron energy distributions by energy groups, thus requiring group average capture cross sections. The figures also illustrate, as histograms, group average cross sections for all radiative capture reactions. Data are from the BUGLE-93 47-group compilation used

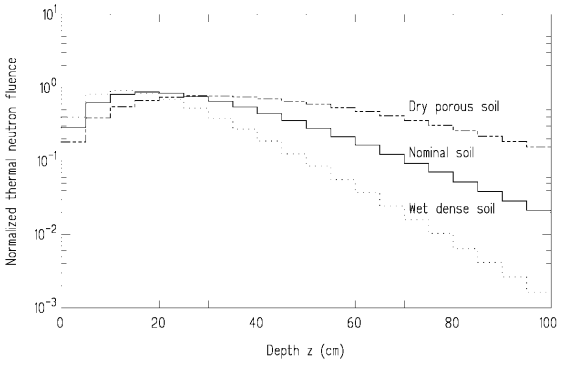

FIGURE 6. THERMAL NEUTRON FLUENCES IN NOMINAL, DRY POROUS, AND WET DENSE SOIL IRRADIATED BY NORMALLY INCIDENT 14-MeV NEUTRONS, COMPUTED BY THE MCNP CODE.

with the TORT and DANTSYS codes.[1] Tabulated data for BUGLE-93 cross sections are given in an earlier report [12]. The group numbering sequence is such that $g = 1$ corresponds to the upper energy for the highest energy group, namely 17.332 MeV. The lowest energy group, the so-called thermal group, corresponds to $g = 47$, with the upper energy $E_{47} = 10^{-7}$ MeV and the lower identified as $E_{48} = 10^{-12}$ MeV. The cross sections are unweighted, that is

$$\sigma_{cg}^{j} = \frac{1}{E_g - E_{g+1}} \int_{E_{g+1}}^{E_g} dE\, \sigma_c^j(E). \tag{5}$$

RESULTS OF MONTE CARLO CALCULATIONS

Detailed results obtained with MCNP for the plane-parallel beam illumination problem have been reported by Faw, *et al.* [12] and are summarized in Figure 6. Because of the strong attenuation of neutrons in the soil, statistical uncertainties at deep penetration were too great to place reliance on Monte Carlo calculations for soil depths in excess of 1 meter. Nevertheless, these results are very important in verifying the results of discrete ordinates calculations. The Monte Carlo calculations closely model the true physical nature of neutron attenuation and results serve as benchmarks for the more abstract discrete ordinates results.

Of great importance in the PGNAA method is the determination of the normalized capture rate by the contaminant element of concern as a function of depth into the soil. The normalized capture rate $A_j(z)$ is the number of neutron captures per unit volume, normalized to unit incident fluence J_o normal to the soil surface and to unit concentration (atoms/cm^3) of the *j*th element in the soil. It is given by

$$\hat{A}_j(z) = \int dE \hat{\Phi}(E,z) \sigma_c^j(E), \tag{6}$$

in which $\sigma_c^j(E)$ is the energy dependent capture cross section for the *j*th element. From MCNP calculations the capture rates for the following elements have been obtained for nominal soils to depths of 150 cm: Al, Ca, Cd, Cl, Cr, Co, Cu, Fe, H, K, Mg, N, Na, Ni, O, P, Pb, Si, Sn, and V. Detailed lists of the normalized capture rates are available [12, 16].

Effective capture cross sections

If the neutron capture rate by a contaminant had to be computed using Equation 6, the PGNAA method would require the energy-dependent fluence $\Phi(E, z)$ to estimate the contaminant profile. Such a requirement would entail huge fluence libraries and considerably complicate the analysis. Fortunately, a major simplification in computing capture rates has been verified in this study.

[1] BUGLE-93 data in Figure 5 are for the single isotope ^{63}Cu. MCNP data are for natural Cu.

Because capture rates for many elements were found to vary with soil depth in constant ratio, an investigation was made of whether one could determine capture rates by simply multiplying the thermal neutron group fluence by an effective capture cross section. The effective cross section is just the ratio of the total capture rate and the thermal-neutron group fluence. The computed effective cross sections obtained in this study are listed in Table 3 and indeed are found to be almost independent of depth in the soil. The uncertainties given in the table are the standard deviations resulting from stochastic variations inherent in Monte Carlo calculations.

Also shown in Table 3 are the E_o = 0.025 eV or 2,200 m/s cross sections σ_o for monoenergetic neutrons given in the DLC140 data collection [17]. It is well known that many neutron capture cross sections vary as the reciprocal of the neutron speed, that is, as $1/\sqrt{E}$. If that is the case, then the expected average cross section for the thermal group (g = 47) with lower energy limit $E_{g+1} = 10^{-6}$ eV and upper limit $E_g = 10^{-1}$ eV (see Table 2) is given, according to Equation 5, by

$$\sigma_c^j = \frac{1}{E_g - E_{g+1}} \int_{E_{g+1}}^{E_g} dE\, \sigma_o^j \sqrt{\frac{E_o}{E}} \cong \sigma_o^j . \qquad (7)$$

The fact that σ_c^j values only slightly exceed σ_o values for all the elements listed except cadmium indicates negligible neutron capture at energies above thermal. Even with cadmium, the effective cross section varies negligibly with the changing neutron energy spectrum as neutrons penetrate more deeply into the soil.

The ability to make use of effective neutron capture cross sections permits a very significant efficiency in the neutron transport calculations required for PGNAA

TABLE 3. EFFECTIVE THERMAL-GROUP NEUTRON CAPTURE CROSS SECTIONS FOR CERTAIN ELEMENTS EXPOSED TO A SPECTRUM OF NEUTRONS CHARACTERISTIC OF THOSE NEUTRONS IN SOIL ARISING FROM NORMALLY INCIDENT 14-MeV NEUTRONS. UNITS ARE BARNS = 10^{-24} cm^2.

	Neutron capture cross section (b)				
Element	Effective[a]	2,200 m/s[b]	Element	Effective[a]	2,200 m/s[b]
Al	0.231 ± 0.005	0.230	N	0.075 ± 0.001	0.075
Ca	0.427 ± 0.008	0.430	Na	0.525 ± 0.010	0.400
Cd	3,420 ± 30	2,450	Ni	4.55 ± 0.03	4.43
Cl	32.8 ± 0.6	33.2	O[c]	0.178 ± 0.003	0.270
Co	38.9 ± 0.9	37.2	P	0.199 ± 0.004	0.180
Cr	3.09 ± 0.02	3.10	Pb	0.180 ± 0.004	0.170
Cu	3.84 ± 0.04	3.79	Si	0.160 ± 0.003	0.160
Fe	2.55 ± 0.02	2.55	Sn	0.643 ± 0.014	0.630
H	0.332 ± 0.006	0.332	U	9.0 ± 1.4	
K	2.09 ± 0.04	2.10	V	5.07 ± 0.09	5.04
Mg	0.063 ± 0.001	0.063			

[a]For application to the energy group from 10^{-11} to 10^{-7} MeV.
[b]For monoenergetic neutrons with speed 2,200 m/s or energy 0.025 eV.
[c]Cross section in units of 10^{-3} b.

of capture gamma data. Discrete ordinates calculations for deep penetration problems, and especially for three-dimensional problems, are significantly less costly in computer time than Monte Carlo calculations. However, the cross-section data resources available for the discrete ordinates calculations are very sparse. For example, data for neutron capture in cadmium, chromium, and other heavy elements are not readily available. However, the cross-section data resources available for the Monte Carlo calculations are rich in capture cross sections. It is thus possible to perform relatively efficient one-dimensional Monte Carlo calculations, the results of which yield effective capture cross sections, which can then be used in three-dimensional discrete ordinates calculations. Preliminary results were reported earlier [12].

RESULTS OF DISCRETE ORDINATES CALCULATIONS

Two discrete-ordinates neutron-transport codes, TORT and DANTSYS, were used to verify earlier Monte Carlo results. These codes, using an entirely different calculational technique and different nuclear data libraries, serve as an excellent check of the MCNP results. In addition, the discrete-ordinates method does not suffer from the statistical uncertainties inherent in the Monte Carlo method and, consequently, is able to determine the neutron fluence at much greater soil depths than could MCNP.

Verification of results

One set of neutron fluence profiles in representative soils was calculated with the MCNP code, which was best suited to calculations for the idealized case of a beam of monoenergetic neutrons normally incident on the soil surface. Such calculations could be done with confidence in the method and with excellent precision in the results provided that depth of penetration was less than about 1 meter. Results of these calculations, reported in Figure 6, formed the basis of subsequent determination of effective capture cross sections.

A second set of neutron fluence profiles was calculated with the TORT code, also for the idealized case of a plane parallel beam normally incidence on the soil. The discrete ordinates calculations offered the advantage of allowing precise transport calculations for soil depths of 2 meters or more. Furthermore, the discrete ordinates method offered the opportunity for two-dimensional transport calculations with much greater precision than could be achieved with Monte Carlo calculations. Such precision would be needed for transmission through the soil of neutrons from a point source above the soil. Comparative results of TORT and MCNP calculations, as evidence of satisfactory code performance, were presented in an earlier report [12].

As efforts to perform two-dimensional calculations began with the TORT code, the DANTSYS code was released. The DANTSYS code was found to be better suited to the type of calculations used in this study, namely transport of neutrons from a point source. A comparison of DANTSYS, TORT, and MCNP results for one-dimensional calculations was made to verify code performance. Figure 7 compares one-dimensional DANTSYS and MCNP results for thermal and fast neutron fluences in nominal soil. It is quite apparent that there is good agreement between Monte Carlo and discrete ordinates calculations over depths

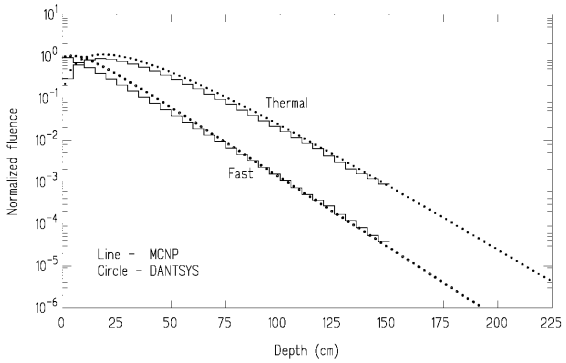

FIGURE 7. COMPARISON OF DANTSYS AND MCNP NORMALIZED FLUENCES IN NOMINAL SOIL RESULTING FROM NORMALLY INCIDENT 14-MeV NEUTRONS ON THE SOIL SURFACE.

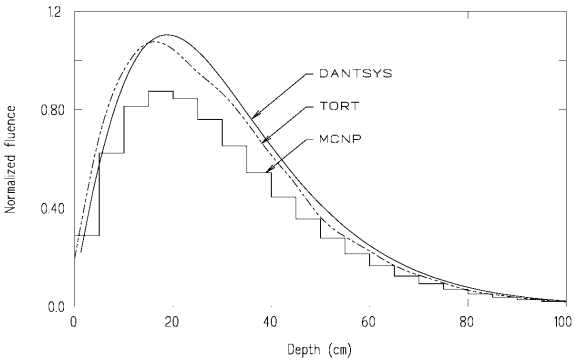

FIGURE 8. COMPARISON OF DANTSYS, TORT, AND MCNP NORMALIZED THERMAL-NEUTRON FLUENCES IN NOMINAL SOIL RESULTING FROM NORMALLY INCIDENT 14-MeV NEUTRONS ON THE SOIL SURFACE.

as great as 1.5 meters and that discrete ordinates calculations are valid at even greater depths. A three-way comparison of one-dimensional results is shown in Figure 8. This graph, on a linear scale, shows excellent agreement between the TORT and DANTSYS results, both differing somewhat from MCNP results. Since the discrete ordinates results agree so well with each other, it appears that there is a degree of systematic uncertainty in the results at shallow depths of penetration. Both TORT and DANTSYS use the same multi-group

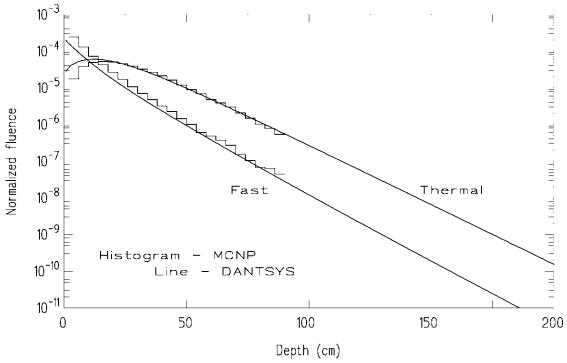

FIGURE 9. COMPARISON OF DANTSYS AND MCNP NORMALIZED FLUENCES IN NOMINAL SOIL RESULTING FROM AN ISOTROPIC 14-MeV NEUTRON SOURCE 15 CM ABOVE THE SOIL SURFACE.

cross-section data and both employ a treatment of the angular distributions of scattered neutrons different from that of the MCNP code. It is thus likely that systematic difference between the Monte Carlo and discrete ordinates results are due to differences in treatment of cross sections and angular distributions. These uncertainties are to be addressed in a subsequent phase of this research.

Two-dimensional calculations for the point-source geometry were also performed using the MCNP and DANTSYS codes. Results are in the form of the thermal and fast neutron fluences as a function of soil depth z and radial distance r from an axis through the source and perpendicular to the soil surface. These fluences are normalized to the number of 14-MeV neutrons released from a point isotropic source 15 cm above the soil surface. The results, expressed as normalized fluence $\tilde{\Phi}(r,z)$, have units of cm^{-2}. Normalized fast-neutron and thermal-neutron fluences along the axis ($r = 0$) are shown in Figure 9. Again, it is quite apparent that there is good agreement between Monte

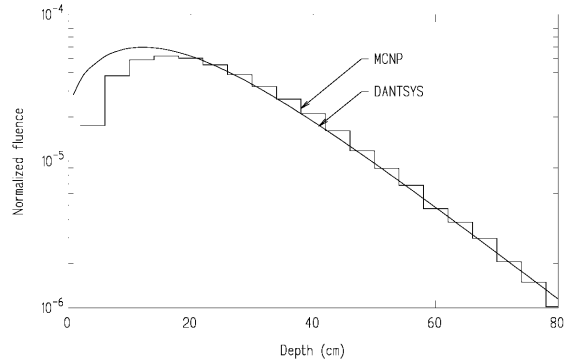

FIGURE 10. COMPARISON OF DANTSYS AND MCNP NORMALIZED FLUENCES IN NOMINAL SOIL RESULTING FROM AN ISOTROPIC 14-MeV NEUTRON SOURCE 15 CM ABOVE THE SOIL SURFACE.

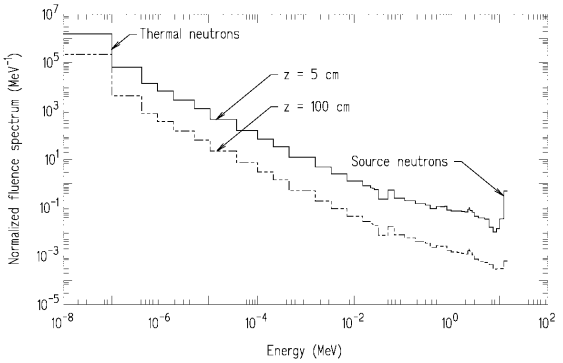

FIGURE 11. ENERGY SPECTRA OF NEUTRONS AFTER ATTENUATION THROUGH 5 AND 100 CM IN NOMINAL SOIL. A UNIT-FLUENCE BEAM OF 14-MeV IS NORMALLY INCIDENT ON THE SOIL SURFACE.

Carlo and discrete ordinates calculations over depths as great as 1.5 meters and that discrete ordinates calculations are valid at even greater depths. Details of the thermal neutron fluences are shown in Figure 10. As in the one-dimensional results, and likely for the same reasons, there is an apparent systematic difference between Monte Carlo and discrete ordinates results for shallow depths of penetration.

Neutron energy spectra

Neutron energy spectra near the surface and at 1 m depth are illustrated in Figure 11 for the case of 14-MeV neutrons normally incident on nominal soil. The normalized spectrum $\ddot{\Phi}(E,z)$, which has units MeV^{-1}, is defined in such a way that $\ddot{\Phi}(E,z)dE$ is the (normalized) fluence of neutrons with energies in the range *dE* about energy *E*. The figure illustrates several points: (1) Except for a constant factor, there is remarkable similarity in the shapes of the spectra at the two extremes of depth. (2) Source neutrons, in the highest energy group are, of course, more plentiful at the shallow depth. (3) Thermal neutrons, in the lowest energy group, dominate the spectra at both depths.[2] (4) Over the broad range of intermediate (epithermal) energies, the energy spectrum of the neutron fluence is inversely proportional to the neutron energy, i.e., $\ddot{\Phi}(E,z) \propto E^{-1}$. This dependence is expected for a medium such as soil within which scattering reactions greatly exceed capture reactions for all but thermal neutrons.

Depth distribution of thermal neutron fluence

The variation of normalized thermal neutron fluence with depth as computed with the DANTSYS is illustrated in Figure 12. Results are shown for nominal soil and for the two extremes of dry porous and wet dense soil. Profiles for dry dense and wet porous soil differ little from the profile for nominal soil. Detailed listings of the thermal fluence as a

[2]The thermal-neutron group fluence $\hat{\Phi}_g(z)$, the integral of $\hat{\Phi}(E,z)$ over energy group 47, also exceeds the fluence for any other energy group except group 2, which comprises source neutrons.

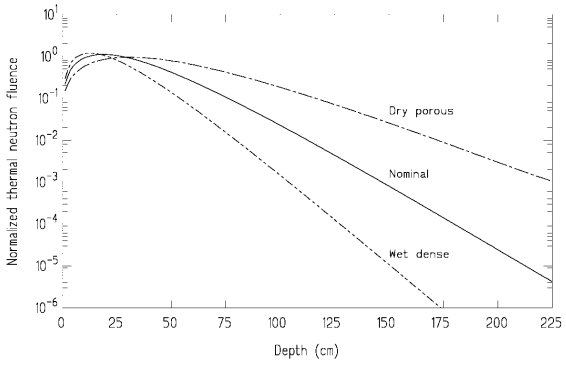

FIGURE 12. NORMALIZED THERMAL NEUTRON FLUENCE IN SOIL RESULTING FROM NORMALLY INCIDENT 14-MeV NEUTRONS ON THE SOIL SURFACE, COMPUTED USING THE DANTSYS CODE.

function of soil depth are presented by Shue and Faw [16] for the five representative soils considered in this study.

To simplify the PGNAA analysis, it is preferable to have a simple approximate function to evaluate the thermal fluence at any soils depth rather than to use tabulated data and interpolation procedures. Consequently, the following rational polynomial approximation was fit to the thermal fluence data calculated by DANTSYS:

$$\log_{10}\left[\hat{\Phi}(E,z)\right] = \frac{a + cz + ez^2}{1 + bz + dz^2}. \quad (8)$$

This approximation was found to fit the data extremely well for all five representative soils. The fit parameters *a* through *e* are given in Table 4.

Two-dimensional fluence profiles

A comprehensive set of two-dimensional calculations was performed using the DANTSYS code for a point source of 14-MeV neutrons located 15.2 cm above the surfaces of soils of representative types. The results, which are expressed as normalized thermal-neutron fluence $\hat{\Phi}(r,z)$, have units of cm^{-2}. Data arrays are too large to be printed. For each type of soil, fluence data are available as a matrix of values for 150 steps in depth up to 250 cm and for 60 steps in radius up to 200 cm.

Figures 13 through 15 are contour plots illustrating the normalized thermal neutron fluence in, respectively, dry porous, wet dense, and nominal soil. Note that the depth and radial scales are different. This was done to illustrate more clearly the variation of intensity with depth. These are for point isotropic sources 15 cm above the surface of the soil and illustrate the effects of

TABLE 4. PARAMETERS FOR THE RATIONAL POLYNOMIAL APPROXIMATION OF THE NORMALIZED THERMAL NEUTRON FLUENCE IN REPRESENTATIVE SOILS RESULTING FROM AN INCIDENT PARALLEL BEAM OF 14-MeV NEUTRONS ON THE SOIL SURFACE.

Soil Type	*a*	*b*	*c*	*d*	*e*
Nominal	-0.6459045	0.0553419	0.0697652	-4.97382E-06	-0.0017017
Dry porous	-0.7241645	0.0306894	0.0417382	3.05685E-06	-0.0006482
Dry dense	-0.7088079	0.0455319	0.0605875	-2.65563E-06	-0.0014170
Wet porous	-0.5800796	0.0531317	0.0658919	-3.32061E-06	-0.0015306
Wet dense	-0.5111661	0.0687761	0.0863490	-1.52629E-06	-0.0030444

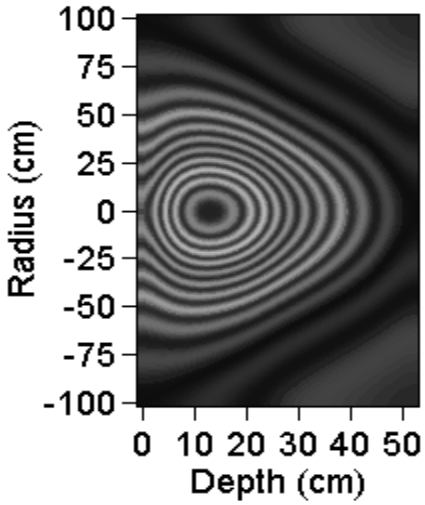

FIGURE 13. CONTOUR PLOT OF THE THERMAL NEUTRON FLUENCE IN NOMINAL SOIL ARISING FROM AN ISOTROPIC 14-MeV NEUTRON SOURCE 15 cm ABOVE THE SOIL SURFACE.

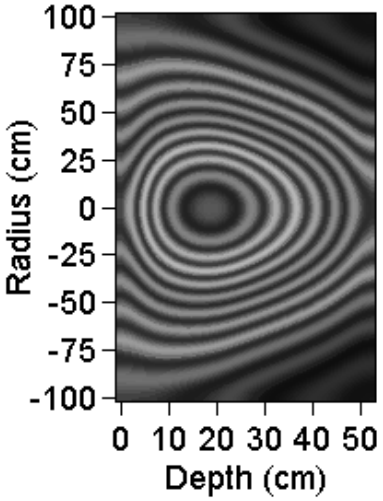

FIGURE 14. CONTOUR PLOT OF THE THERMAL NEUTRON FLUENCE IN DRY POROUS SOIL ARISING FROM AN ISOTROPIC 14-MeV NEUTRON SOURCE 15 cm ABOVE THE SOIL SURFACE.

geometric attenuation (the inverse-square law) as well as the rapid thermalization of neutrons, which is attributable largely to the presence of hydrogen in the water content of the soil. One sees in these plots how the fluence peaks strongly at depths on the order

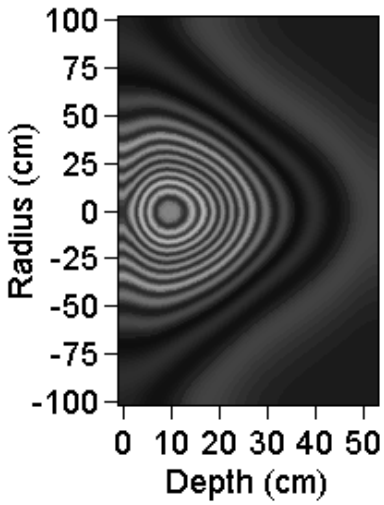

FIGURE 15. CONTOUR PLOT OF THE THERMAL NEUTRON FLUENCE IN WET DENSE SOIL ARISING FROM AN ISOTROPIC 14-MeV NEUTRON SOURCE 15 CM ABOVE THE SOIL SURFACE.

of 10 cm for wet dense soil to 20 cm for dry porous soil. Clearly, the PGNAA method applies more sensitively to soil contaminants within the upper half meter or so of soil.

FUTURE WORK

Work is underway in computing fluence profiles for two additional neutron sources of potential interest in PGNAA. These are the ^{252}Cf spontaneous-fission source and the ^{241}Am/Be (α, n) source. An investigation is also underway into the combination of PGNAA techniques with imaging techniques similar to those used in nuclear medicine. A gamma-ray camera would be used to generate plane images of buried objects or images of finite accumulations of contaminants. It is expected that this work will lead to the use of tomographic methods for three-dimensional imaging.

REFERENCES

1. J.K. Shultis, R.E. Faw, and F.A. Khan, Mathematical Models and Analysis for PGNAA of Soil Contamination, HSRC-94-02-10, Kansas State University, Manhattan, Kansas, 1996.

2. T.V. Congedo, F.H. Ruddy, and D.F. McLaughlin, Neutron Transport Modeling in Support of Prompt Gamma Neutron Activation for Environmental Analysis, 937TD1-PGEXT-P2, Westinghouse Science and Technology Center, 1993.

3. R.H. Ruddy, T.V. Congedo, J.G. Seidel, J.L. Gonzales, and D.H. Weigle, In-Situ Characterization of Hazardous Contaminants using Prompt Gamma Neutron Activation Analysis, 93-7TD1-PGEXT-P1, Westinghouse Science and Technology Center, 1993.

4. D.H. Weigle, Contamination Detection using Prompt Gamma Neutron Activation Analysis, Personal correspondence with Scientific Ecology Group, Inc., 1993.

5. D.H. Weigle, Subsurface, Simultaneous, Multi-Elemental Analysis of Contaminated Soil, prepared for presentation at the 1993 AIChE Summer International Meeting by Scientific Ecology Group, Inc., 1993.

6. J.F. Breismeister (Ed.), MCNP - A General Monte Carlo N-Particle Transport Code, Technical Report, Los Alamos National Laboratory, Los Alamos, New Mexico, 1987.

7. W.A. Rhoades and R.L. Childs, The TORT Three-Dimensional Discrete Ordinates Neutron/Photon Transport Code, Technical Report, Oak Ridge National Laboratory, Oak Ridge, Tennessee, 1987.

8. R.E. Alcouffe, Diffusion synthetic acceleration methods for the diamond-difference discrete-ordinates equations, Nuclear Science and Engineering, 64 (1977) 344.

9. W.L. Filippone and R.E. Alcouffe, The Sn/Monte Carlo response matrix hybrid method, Nuclear Science and Engineering, 100 (1988) 209-217.

10. W.F. Filippone, R.S. Baker, and R.E. Alcouffe, The Monte Carlo/Sn hybrid method with orthogonal interface basis vectors, Joint Intl. Conf. on Math. Methods and Supercomputing in Nuclear Applications, Karlsruhe, Germany, 1993, vol. 2, pp. 714-724, 1993.

11. R.E. Alcouffe, R.S. Baker, F.W. Brinkley, D.R. Marr, R.D. O'Dell, and W.F. Walters, DANTSYS: A Diffusion Accelerated Neutral Particle Transport Code System, Technical Report, Los Alamos National Laboratory, Los Alamos, New Mexico, 1995.

12. R.E. Faw, J.K. Shultis, B.C. Letellier, S.L. Shue, and F.A. Khan, First Quarter Progress Report: PGNAA Applications in Characterization of Contaminated Soils, HSRC-94-02-06, Kansas State University, Manhattan, Kansas, 1995.

13. A.B. Chilton, J.K. Shultis, and R.E. Faw, Principles of Radiation Shielding, Prentice-Hall, Englewood Cliffs, New Jersey, 1984.

14. J.J. Duderstadt and L.J. Hamilton, Nuclear Reactor Analysis, John Wiley and Sons, NY, 1976.

15. S.L. Shue, Use of the Discrete Ordinates Code DANTSYS in Neutron Transport Calculations, HSRC-94-02-07, Kansas State University, Manhattan, Kansas, 1996.

16. S.L. Shue and R.E. Faw, Penetration of 14 MeV Neutrons into Representative Soils, HSRC-94-02-09, Kansas State University, Manhattan, Kansas, 1996.

17. M.A. Lone, R.A. Leavitt, and D.A. Harrison, Prompt gamma rays from thermal neutron capture, Atomic Data and Nuclear Data Tables, 26 (1981) 551-559; data available as DLC-140, Prompt Gamma Rays from Thermal-Neutron Capture, Radiation Shielding Information Center, Oakridge National Laboratory, Oak Ridge, Tennessee.